Serial propagation of distinct strains of Aβ prions from Alzheimer's disease patients

Joel C. Watts[a,b,1], Carlo Condello[a], Jan Stöhr[a,b], Abby Oehler[c], Joanne Lee[a], Stephen J. DeArmond[a,c], Lars Lannfelt[d], Martin Ingelsson[d], Kurt Giles[a,b], and Stanley B. Prusiner[a,b,2]

[a]Institute for Neurodegenerative Diseases and Departments of [b]Neurology and [c]Pathology, University of California, San Francisco, CA 94143; and [d]Department of Public Health/Geriatrics, Uppsala University, 751 85 Uppsala, Sweden

An increasing number of studies argues that self-propagating protein conformations (i.e., prions) feature in the pathogenesis of several common neurodegenerative diseases. Mounting evidence contends that aggregates of the amyloid-β (Aβ) peptide become self-propagating in Alzheimer's disease (AD) patients. An important characteristic of prions is their ability to replicate distinct strains, the biological information for which is enciphered within different conformations of protein aggregates. To investigate whether distinct strains of Aβ prions can be discerned in AD patients, we performed transmission studies in susceptible transgenic mice using brain homogenates from sporadic or heritable (Arctic and Swedish) AD cases. Mice inoculated with the Arctic AD sample exhibited a pathology that could be distinguished from mice inoculated with the Swedish or sporadic AD samples, which was judged by differential accumulation of Aβ isoforms and the morphology of cerebrovascular Aβ deposition. Unlike Swedish AD- or sporadic AD-inoculated animals, Arctic AD-inoculated mice, like Arctic AD patients, displayed a prominent Aβ38-containing cerebral amyloid angiopathy. The divergent transmission behavior of the Arctic AD sample compared with the Swedish and sporadic AD samples was maintained during second passage in mice, showing that Aβ strains are serially transmissible. We conclude that at least two distinct strains of Aβ prions can be discerned in the brains of AD patients and that strain fidelity was preserved on serial passage in mice. Our results provide a potential explanation for the clinical and pathological heterogeneity observed in AD patients.

neurodegeneration | bioluminescence imaging | seeding | proteinopathies

Alzheimer's disease (AD) is the most common human neurodegenerative disease, and it is characterized by the accumulation of extracellular amyloid plaques composed of aggregated amyloid-β (Aβ) peptide as well as intracellular neurofibrillary tangles composed of aggregated and hyperphosphorylated tau protein in the brain. The Aβ peptide is generated by the sequential cleavage of the amyloid precursor protein (APP) by β- and γ-secretase enzymes. The amyloid cascade hypothesis posits that the accumulation and subsequent deposition of Aβ in the brain are the initiating pathological events in AD that lead to the downstream aggregation of tau (1). Although most AD cases are sporadic, a minority results from mutations in the genes encoding APP or γ-secretase components.

Mounting evidence argues that the progressive nature of AD as well as many other neurodegenerative illnesses may stem from the formation and subsequent spread of self-propagating, β-sheet–rich protein conformations (i.e., prions) in the brain (2–4). The term prion, derived from the words "protein" and "infectious," was introduced to define a novel pathogen lacking nucleic acids (5). Because the mechanism of prion propagation was shown to involve template-directed conformational change, the prion paradigm was recognized to apply more broadly in biology, including non-Mendelian phenotypic inheritance in yeast (6) and maintenance of synapse-specific changes in neurons (7). Diverse studies have converged to argue that prions, formed from normal proteins, cause many, if not

most, neurodegenerative diseases (8). Some investigators prefer to use other terms for these self-propagating protein aggregates, including prion-like protein aggregates, prionoids, and proteopathic seeds (9, 10).

A wealth of studies argues that the formation of Aβ prions is involved in the pathogenesis of AD. In AD, cerebral Aβ deposition follows a stereotypical progression, in which the neocortex is targeted first, followed by spreading to subcortical regions of the brain (11). Moreover, inoculation of susceptible transgenic (Tg) mice or rats expressing mutant or WT human APP with brain homogenate containing Aβ aggregates, purified Aβ amyloid fibrils, or synthetic Aβ aggregates induced widespread cerebral Aβ deposition, revealing that Aβ aggregates are self-propagating and hence, prions (12–17).

An important characteristic of prions is their ability to replicate distinct strains, which can be distinguished by their transmission behavior as well as their biochemical and pathogenic properties. Prion strain-specific biological information is enciphered within different conformations of protein aggregates (18–20). Distinct conformations of Aβ aggregates have been described as formed either spontaneously from synthetic Aβ (21–23) or after seeding of synthetic Aβ by Aβ aggregates from AD brains (24, 25). Furthermore, AD is a clinically heterogeneous disease (26), which could potentially be explained by the existence of multiple Aβ strains.

Based on the observation that different mutations in the human prion protein (PrP) encipher distinct strains of PrP prions (19), we hypothesized that heritable AD caused by different APP mutations (particularly mutations that result in the production of

Significance

The amyloid-β (Aβ) peptide, which plays a central role in Alzheimer's disease (AD) pathogenesis, exhibits many properties that are reminiscent of prions (self-propagating proteins that cause neurodegenerative disorders, such as mad cow disease). In the human prion diseases, distinct strains of prions can be distinguished, and therefore, we asked whether different strains of Aβ aggregates might exist in the brains of AD patients. Inoculation of transgenic mice with brain samples from patients with two different heritable forms of AD produced two distinct patterns of cerebral Aβ deposition, and these differences were maintained on serial passage. We conclude that distinct strains of Aβ can be discerned in AD patients, which may help to explain the clinical heterogeneity observed in the disease.

NEUROSCIENCE

mutant Aβ) might result in the formation of distinct Aβ prion strains. The Arctic mutation in APP (E693G) occurs within the sequence of Aβ (E22G), causes enhanced Aβ protofibril formation, produces distinct fibril morphology, and results in a distinct AD pathology (27–30). In contrast, the Swedish mutation (K670M/N671L) occurs outside the Aβ sequence but results in the overproduction of WT Aβ and typical AD pathology (31–33). Here, we report that brain homogenates from Arctic and Swedish AD patients induced distinct disease phenotypes after multiple passages in susceptible Tg mice, suggesting that distinct Aβ strains form in the brains of AD patients.
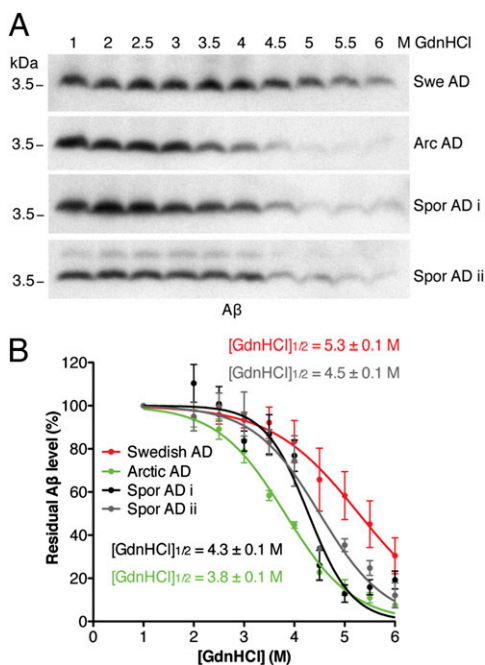
Results

To determine whether the brains from an Arctic AD patient and a Swedish AD patient contain distinct conformations of Aβ aggregates, we performed conformational stability assays, which have been used to distinguish different strains of PrP prions (34). Brain homogenates prepared from AD patients were subjected to increasing concentrations of guanidine hydrochloride (GdnHCl) to determine the resistance of aggregates to denaturation. Samples were then digested with proteinase K (PK), and the residual fraction of PK-resistant Aβ was analyzed by Western blotting (Fig. 1A). We then calculated $[GdnHCl]_{1/2}$ values (the GdnHCl concentration at which 50% of Aβ is denatured) and found that the Aβ aggregates in the Arctic AD sample were significantly less resistant to GdnHCl denaturation than the Aβ aggregates in the Swedish AD sample (Fig. 1B), arguing that they are conformationally distinct. We also analyzed brain homogenates from two sporadic cases of AD, which yielded intermediate conformational stabilities.

To test if the distinct Aβ conformations in the brains of Arctic and Swedish AD patients are self-propagating, we performed
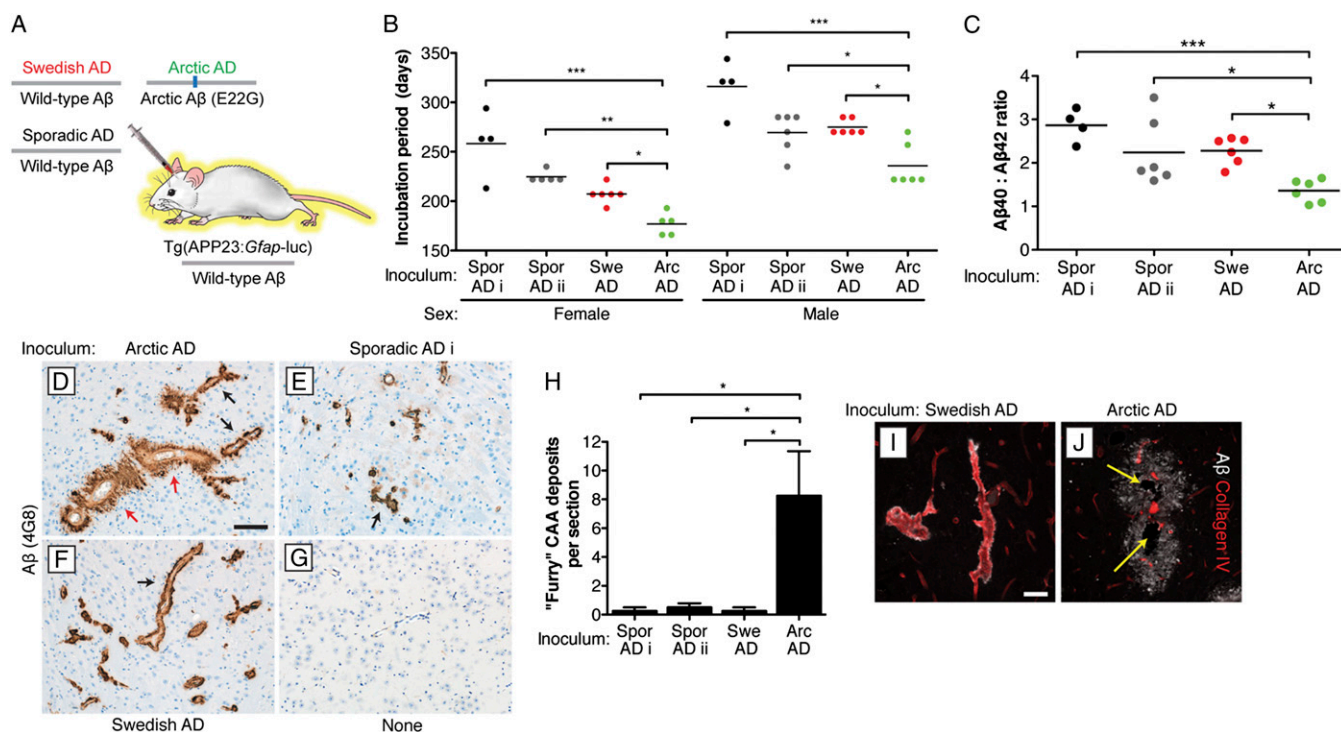

Fig. 1. The Aβ aggregates in Swedish and Arctic AD patient brains are conformationally distinct. (A) Representative immunoblots and (B) denaturation curves of residual PK-resistant Aβ levels after conformational stability assays of Aβ species present in brain homogenates from Swedish, Arctic, or sporadic AD patients (n = 3 technical replicates each). The $[GdnHCl]_{1/2}$ value for Arctic Aβ aggregates was significantly lower than that of Swedish Aβ aggregates ($P < 0.001$), sporadic AD case i Aβ aggregates ($P < 0.01$), and sporadic AD case ii Aβ aggregates ($P < 0.001$), indicative of a distinct aggregate conformation. Aβ levels were detected with the 6E10 antibody. Arc, Arctic; Spor, sporadic; Swe, Swedish.

transmission studies in bigenic Tg(APP23:Gfap-luc) mice (Fig. 2A) that express a Swedish mutant human APP transgene that produces WT Aβ peptide as well as a luciferase reporter under the control of the GFAP promoter (35, 36). This system permits the kinetics of induced cerebral Aβ accumulation to be monitored in living animals using bioluminescence imaging (BLI) of astrocytosis stimulated by the deposition of Aβ in amyloid plaques (14). Tg(APP23:Gfap-luc) mice were intracerebrally inoculated with brain homogenates from the four AD cases as well as a control homogenate from an age-matched individual free of any neurodegenerative illnesses. Levels of both formic acid-extractable and PK-resistant Aβ were much higher in the AD homogenates compared with the control homogenate (Table S1 and Fig. S1A). Inoculation with each of the AD homogenates accelerated the onset of the brain BLI signal increase compared with inoculation with the control homogenate (Fig. S1A). Moreover, Aβ levels, cerebral Aβ deposition, and Aβ plaque-associated astrocytic gliosis were significantly greater in the mice inoculated with AD brain homogenate compared with control-inoculated and uninoculated animals (Fig. S1 B–R), indicating that the four AD homogenates contained Aβ prions.

Remarkably, the Arctic AD sample induced a distinct disease phenotype in the bigenic mice that could be distinguished from both the Swedish and sporadic AD inocula. Incubation periods for Aβ aggregate-containing samples on inoculation into Tg (APP23:Gfap-luc) mice can be assigned using BLI by measuring the time interval from inoculation to when a sustained increase in brain bioluminescence is observed (16). For these calculations, male and female mice were considered separately, because the kinetics of Aβ accumulation in Tg(APP23) mice are sex-dependent (37). The incubation period for the Arctic AD sample in both male and female mice was significantly shorter than for the other AD samples (Fig. 2B), despite lower levels of formic acid-extractable Aβ in the inoculum (Table S1). Furthermore, the ratio of Aβ40 to Aβ42 in the Arctic AD-inoculated mice was significantly lower than in the mice inoculated with the other three samples (Fig. 2C). Different Aβ peptide ratios were also observed after inoculation of Tg(APP23) mice with brain extracts from two different Tg mouse models of AD (38).

Despite harboring parenchymal Aβ deposits of similar morphology to other AD-inoculated mice (Fig. S1), the Arctic AD-inoculated animals showed a striking difference in the morphology of Aβ cerebral amyloid angiopathy (CAA) in the thalamus. Much of the thalamic CAA in Arctic AD-inoculated mice at 330 d postinoculation appeared furry in nature, with Aβ deposits radiating outward from the blood vessels (Fig. 2D and Fig. S2A). A similar CAA morphology was observed in the thalamus of Tg mice expressing Arctic mutant APP (39). In contrast, mice inoculated with sporadic AD case i, Swedish AD, brain homogenate from an aged Tg(APP23) mouse, Aβ fibrils purified from Tg(APP23) mice (16), or synthetic Aβ(1–40) peptide as well as 635-d-old uninoculated mice all exhibited a similar pattern of CAA: a thin, compact layer of Aβ deposition surrounding blood vessels (Fig. 2 E and F and Fig. S2 B–E). Interestingly, mice inoculated with sporadic AD case ii exhibited both CAA morphologies (Fig. S2 F and G). Uninoculated Tg (APP23:Gfap-luc) mice at 390 d of age did not exhibit any spontaneous CAA in the thalamus (Fig. 2G). Significantly greater numbers of furry Aβ CAA deposits were observed in the Arctic AD-inoculated animals (Fig. 2H). Because the incubation periods for female mice inoculated with Arctic AD and purified Aβ fibrils were similar (~170 d) (16), the unique furry vessel phenotype in Arctic AD-inoculated animals cannot be attributed to faster Aβ replication kinetics. No CAA was found in any of the inoculated mice at 33 d postinoculation (Fig. S3), indicating that the induced CAA was not composed of residual inoculated material. Staining for collagen IV, which labels the basement membrane of blood vessels, revealed that many of the thalamic

www.manaraa.com

Fig. 2. Arctic AD brain homogenate induces a distinct disease in Tg(APP23:*Gfap*-luc) mice. (*A*) Schematic of the inoculation experiment in bigenic Tg(APP23:*Gfap*-luc) mice, which produce WT Aβ peptide. (*B*) Incubation periods, determined by BLI, were significantly lower in mice inoculated with Arctic AD than in mice inoculated with Swedish or sporadic AD. Points are from individual mice; mean incubation periods are indicated by the horizontal lines. Female and male mice are shown separately because of sex differences in the kinetics of Aβ deposition in Tg(APP23) mice. (*C*) The ratio of Aβ40 to Aβ42 was significantly lower in mice inoculated with Arctic AD than in mice inoculated with Swedish or sporadic AD. (*D*–*G*) Aβ CAA in the thalamus of female mice at 330 d postinoculation (dpi) with the indicated brain homogenates. Whereas mice inoculated with Swedish or sporadic AD case i exhibited a thin, compact layer of Aβ deposition surrounding blood vessels (black arrows), many of the Aβ-positive blood vessels in Arctic AD-inoculated animals appeared furry in nature (red arrows). (*G*) The brain section from an uninoculated mouse at 390 d of age is shown as a control. (Scale bar: *D*–*G*, 100 μm.) (*H*) Significantly greater numbers of furry vessels were observed in the thalamus of mice inoculated with Arctic AD than in mice inoculated with Swedish or sporadic AD. Quantification was done by visual inspection of stained furry vessels in immunohistochemical slides of inoculated mice (*n* = 4 each). (*I* and *J*) Double labeling of Aβ (white) and collagen IV (red) in the thalamus of Swedish AD- and Arctic AD-injected female mice at 330 dpi. The blood vessels surrounded by furry Aβ deposits in Arctic AD-inoculated animals were atrophic (yellow arrows). (Scale bar: *I* and *J*, 50 μm.) For *D*–*J*, Aβ was labeled using the 4G8 antibody. Arc, Arctic; Spor, sporadic; Swe, Swedish. *$P < 0.05$; **$P < 0.01$; ***$P < 0.001$.

blood vessels surrounded by the furry Aβ deposits in Arctic AD-inoculated mice, but not Swedish AD-inoculated mice, were undergoing atrophy (Fig. 2 *I* and *J*).

A key feature that distinguishes Arctic AD cases from most sporadic AD cases and cases of heritable AD in which the mutation does not occur within the sequence of Aβ is the preferential deposition of Aβ38 peptide, particularly surrounding blood vessels (40). Indeed, PK-resistant Aβ38 was abundant in the Arctic AD sample and present in sporadic AD case ii but absent in the Swedish AD and sporadic AD case i samples (Fig. 3*A*). We used mAb BA1-13, which is specific for the Aβ peptide ending at residue 38 (Fig. S4*A*), to assess Aβ38 deposition in AD-inoculated mice. Mice inoculated with either Arctic or Swedish AD samples showed similar levels of formic acid-extractable Aβ38 in their brains (Fig. S4*B*) and amyloid plaques (Fig. S4 *C* and *D*). However, abundant Aβ38-positive CAA within the thalamus was observed in mice inoculated with Arctic Aβ (Fig. 3*B*) but not in mice inoculated with Swedish AD or sporadic AD case i. Mice inoculated with sporadic AD case ii also exhibited some thalamic Aβ38-positive CAA (Fig. 3*C*). The quantity of Aβ38-positive blood vessels in the thalamus, leptomeninges, and the frontal cortex was significantly greater in Arctic AD-inoculated mice compared with sporadic AD- and Swedish AD-injected mice (Fig. 3*D* and Fig. S4 *E* and *F*).

To confirm these findings, we analyzed a second cohort of Arctic AD- and Swedish AD-inoculated mice by quantitative confocal fluorescence microscopy using a different Aβ38-specific antibody (7-14-4) (Fig. S4*A*). Significantly higher levels of Aβ38 staining were observed in thalamic blood vessels in Arctic AD-inoculated mice compared with Swedish AD-inoculated animals (Fig. 3 *E*–*G*). Moreover, codeposition of Aβ38 and Aβ40 peptides in thalamic blood vessels was observed in mice inoculated with Arctic AD or sporadic AD case ii but not in mice inoculated with Swedish AD, sporadic AD case i, or other Aβ aggregate-containing preparations (Fig. 3 *H* and *I* and Fig. S5 *A*–*G*). Inoculation of mice with brain homogenate from aged Tg(APP23) mice, which also contained elevated levels of PK-resistant Aβ38 peptide (Fig. S5 *H*–*J*), did not result in Aβ38-positive CAA within the thalamus (Fig. S5*E*), suggesting that the conformation of Aβ in the inoculum, not the absolute levels of Aβ38, determines the phenotype in inoculated mice. These observations argue that the Arctic AD sample induced the preferential deposition of Aβ38 in blood vessels in mice that do not express the Arctic mutation. That induced Aβ38 deposition within plaques was observed in mice injected with Swedish or Arctic AD (Fig. S4 *C* and *D*), despite the absence of PK-resistant Aβ38 in the Swedish AD inoculum (Fig. 3*A*), may reflect a predisposition of Tg(APP23) mice to depositing Aβ38 in amyloid plaques (Fig. S5*I*).

An important characteristic of prion strains composed of PrP is that their properties are generally maintained after repeated passages in mice. To test if Aβ strains can also be serially
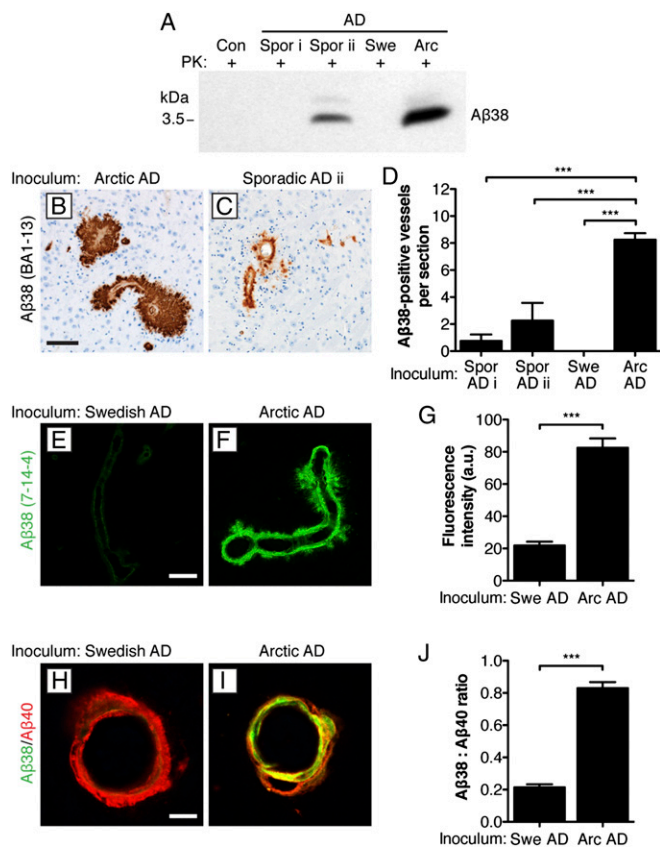
Fig. 3. CAA with Aβ38 deposition after inoculation of Tg(APP23:*Gfap*-luc) mice with Arctic AD but not Swedish AD brain homogenate. (*A*) Relative levels of PK-resistant Aβ38 in the various inocula as detected by immunoblotting using the Aβ38-specific antibody 7-14-4. (*B* and *C*) Deposition of Aβ38 (BA1-13 antibody) within furry thalamic blood vessels in female Tg(APP23:*Gfap*-luc) mice at 330 d postinoculation (dpi) with either (*B*) Arctic AD or (*C*) sporadic AD case ii brain homogenate. (Scale bar: *B* and *C*, 100 μm.) (*D*) Quantification by visual inspection of immunohistochemical slides of Aβ38-positive (BA1-13 antibody) thalamic blood vessels in mice inoculated with the indicated brain homogenates (*n* = 4 each). Significantly more Aβ38 deposits were observed in the Arctic AD-inoculated animals. (*E* and *F*) Deposition of Aβ38 (7-14-4 antibody) within thalamic blood vessels in a second cohort of Tg (APP23:*Gfap*-luc) mice at 330 dpi with either (*E*) Swedish AD or (*F*) Arctic AD brain homogenate. (Scale bar: *E* and *F*, 50 μm.) (*G*) Quantification by quantitative confocal fluorescence microscopy of the relative amount of Aβ38 staining (7-14-4 antibody) in thalamic blood vessels in mice inoculated with Swedish AD (*n* = 51 total blood vessels from three mice) or Arctic AD (*n* = 31 total blood vessels from three mice) brain homogenate. Significantly higher levels of Aβ38 deposition were observed in the Arctic AD-inoculated animals. (*H* and *I*) Double labeling of Aβ38 (7-14-4 antibody; green) and Aβ40 (11A50-B10 antibody; red) in the thalamus of female mice at 330 dpi with either (*H*) Swedish AD or (*I*) Arctic AD brain homogenate. (Scale bar: *H* and *I*, 15 μm.) (*J*) Quantification of the ratio of Aβ38 (7-14-4 antibody) to Aβ40 (11A50-B10 antibody) staining in thalamic blood vessels in mice inoculated with Swedish AD (*n* = 51 total blood vessels from three mice) or Arctic AD (*n* = 31 total blood vessels from three mice) brain homogenate. Significantly higher ratios were observed in the Arctic AD-inoculated animals. Arc, Arctic; Con, control; Spor, sporadic; Swe, Swedish. ***$P < 0.001$.

propagated in mice, we performed a second passage experiment. In these experiments, both the passaged Swedish and Arctic inocula contained identical Aβ sequences, because they both underwent initial passage in Tg(APP23:*Gfap*-luc) mice producing WT Aβ peptide (Fig. 4*A*). On second passage, the Swedish and Arctic AD samples as well as sporadic AD case i accelerated the onset of the brain BLI signal increase and the elevation of cerebral Aβ deposition compared with passaged

control brain homogenate (Fig. S6). Second passage of all AD samples resulted in incubation periods similar to their respective first passages, with the Arctic AD inoculum showing the shortest incubation periods (Fig. 4*B*). Similar to first passage, furry Aβ CAA deposits were observed in the thalamus of mice inoculated with the passaged Arctic AD sample but not in mice inoculated with the passaged Swedish AD sample (Fig. 4 *C–E*). Likewise, mice inoculated with the passaged Arctic AD sample, but not mice inoculated with the passaged Swedish or sporadic AD samples, exhibited prominent CAA deposition of Aβ38 in the thalamus (Fig. 4 *F–H*) and other areas of the brain (Fig. S7 *A and B*) as well as codeposition of Aβ38 and Aβ40 in thalamic blood vessels (Fig. 4 *I* and *J*). Levels of formic acid-extractable Aβ38 were not significantly different in mice inoculated with the passaged Arctic or Swedish AD samples (Fig. S7*C*).

Discussion

In the studies reported here, we found evidence for distinct strains of Aβ prions in brain homogenates prepared from patients with heritable AD. At least certain properties of the Aβ prion strains, such as the relative amounts of cerebrovascular Aβ38 deposition, were maintained after multiple passages in Tg mice. The existence of distinct Aβ strains and their ability to be serially propagated in mice contend that the Aβ aggregates in the brains of AD patients show all of the attributes of prions.

By melting the conformation of Aβ, we found that the Aβ prions in the brain of a patient carrying the Arctic mutation and producing mutant Aβ (E22G) were substantially less resistant to GdnHCl denaturation than those in the brain of a patient with the Swedish mutation, which does not alter the sequence of WT Aβ. We note that Arctic AD patients are heterozygous for the mutation, resulting in a mixture of WT and mutant Aβ peptides in the brain. Although we did not determine the allelic origin of the protease-resistant Aβ isoforms, studies of mutant PrPs may be informative: mutant PrPs in patients harboring the P102L, D178N, or E200K mutations were preferentially converted into the PrP^Sc isoform (41–43). Assuming that Arctic Aβ was preferentially converted into prions as manifest by protease resistance, it seems likely that WT Aβ did not form prions, because a monophasic melting curve was observed (Fig. 1*B*). If WT Aβ in Arctic AD patients had become a prion and adopted a conformation similar to the WT Aβ prions in the brain of the Swedish AD patient, then the melting curve should have been biphasic. Alternatively, WT Aβ may have adopted the same conformation as Arctic mutant Aβ.

The analysis of mutant and WT Aβ prions is further complicated by heterogeneous γ-secretase cleavage that generates Aβ peptides varying in length from 37 to 43 aa (44). Each of these peptides is likely to possess a different thermodynamic landscape with respect to conversion into a prion. The difficulties surrounding studies of Aβ prion strains are highlighted by a study using Tg(APP23) and Tg(APPPS1) mice; the former produces much more Aβ40 than Aβ42, whereas the latter produces the opposite (38). In our AD-inoculated mice, the most prominent strain-specific differences, including the relative amount of Aβ38 deposition, were observed in cerebral blood vessels but not parenchymal amyloid plaques. However, this difference was not inherent to the Tg(APP23) line, because mice inoculated with distinct strains of synthetic Aβ prions exhibited strain-specific differences in the ratios of Aβ40 and Aβ42 within amyloid plaques (45).

Our studies suggest that the Arctic AD mutation may encode a strain of Aβ prions that is distinct from that enciphered by the Swedish mutation, although this result will need to be confirmed using additional cases. Based on our transmission studies, it seems likely that the Aβ strains present in the Swedish AD and sporadic AD case i samples are similar and that the sporadic AD case ii sample contains a mixture of the Swedish-like and Arctic-like

www.manaraa.com
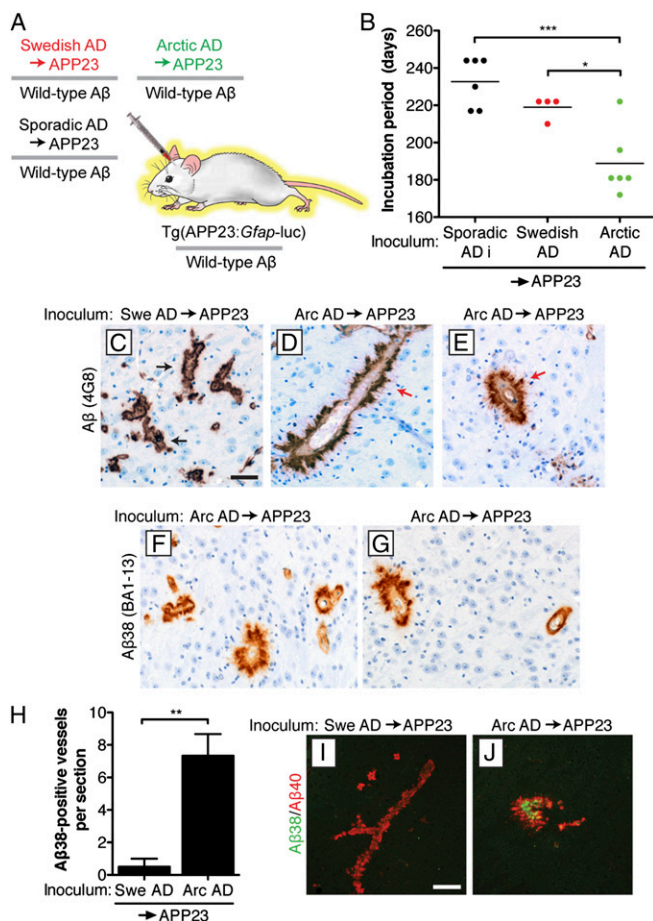
Fig. 4. Aβ strain properties are maintained on serial transmission in Tg (APP23:*Gfap*-luc) mice. (*A*) Schematic of the second passage of AD samples in Tg(APP23:*Gfap*-luc) mice. The passaged Arctic, Swedish, and sporadic AD inocula are composed of WT Aβ peptide. (*B*) The incubation periods were significantly shorter for the passaged Arctic AD sample than for the passaged sporadic AD case i and Swedish AD samples. Points are from individual female mice; mean incubation periods are indicated by the horizontal lines. (*C*–*E*) Aβ CAA in the thalamus of female mice at 330 d postinoculation (dpi) with the indicated passaged brain homogenates. Whereas mice inoculated with passaged Swedish AD exhibited a thin, compact layer of Aβ deposition (4G8 antibody) surrounding blood vessels (black arrows), many of the Aβ-positive blood vessels in animals inoculated with passaged Arctic AD appeared furry in nature (red arrows). (*F* and *G*) Thalamic CAA with Aβ38 deposition (BA1-13 antibody) was observed in two distinct female Tg(APP23:*Gfap*-luc) mice at 330 dpi with the passaged Arctic AD sample. (Scale bar: *C*–*G*, 50 μm.) (*H*) Quantification of Aβ38-positive (BA1-13 antibody) thalamic blood vessels in mice inoculated with the passaged Swedish ($n = 4$) or Arctic AD ($n = 6$) samples. (*I* and *J*) Double labeling of Aβ38 (BA1-13 antibody; green) and Aβ40 (11A50-B10 antibody; red) in the thalamus of female mice at 330 dpi with passaged Swedish or Arctic AD samples. Only the mice inoculated with the passaged Arctic AD sample exhibited codeposition of Aβ38 and Aβ40 peptides. (Scale bar: *I* and *J*, 100 μm.) Arc, Arctic; Swe, Swedish. *$P < 0.05$; **$P < 0.01$; ***$P < 0.001$.

strains. Interestingly, the Dutch mutation in Aβ (E22Q) (46), which occurs at the same residue as the Arctic mutation, leads almost exclusively to cerebrovascular Aβ deposition and cerebral hemorrhages, implying the existence of additional Aβ strains and suggesting that residue 22 in Aβ may be critical for determining the conformation of Aβ prions. However, mutations within the Aβ peptide sequence may not be necessary for the genesis of distinct strains, because different conformations of Aβ aggregates have been observed in two different cases of sporadic AD (25). Moreover, different subtypes of sporadic AD, such as rapidly

progressive AD (47), may stem from the propagation of unique strains of WT Aβ prions in the brain.

Because the Tg(APP23:*Gfap*-luc) mice used herein produce WT Aβ peptide, we conclude that the conformation of Aβ aggregates (not the presence of a mutation per se) enciphers the properties of Aβ strains. These findings parallel the maintenance of strain-specified properties observed on transmission of different inherited forms of human PrP prion disease, each expressing a different mutant PrP molecule, to Tg mice expressing chimeric mouse/human PrP (19). The phenotypic differences observed from the Arctic and Swedish AD transmissions may be caused by the Arctic mutation favoring the formation of a self-propagating Aβ conformation in which Aβ38 is stabilized, leading to its accumulation and deposition in the brain. However, a similar conformation may infrequently arise spontaneously in the absence of a mutation in Aβ, which was observed with sporadic AD case ii.

Distinct self-propagating strains of protein aggregates have also recently been described for both the human synucleinopathies and tauopathies (48–50). Experimental transmission of multiple system atrophy to Tg mice revealed a particularly aggressive strain of WT α-synuclein prions (49). The existence of multiple prion strains causing neurodegenerative diseases poses a challenge for the development of therapeutics. Studies with PrP prions have revealed that therapeutic compounds identified using mouse-passaged strains were efficacious against mouse and chronic wasting disease prions but not against human strains (51). Because the conformation of Aβ aggregates in Tg mice seems distinct from that in AD patients (52), the translational use of such mouse models for anti-Aβ therapeutics seems questionable. Our ability to propagate distinct AD-associated Aβ strains in the brains of Tg(APP23:*Gfap*-luc) mice may, therefore, provide a superior tool for assessing drug efficacy. More importantly, heterogeneity in Aβ aggregate conformations suggests that passive Aβ immunotherapy approaches for treating AD may only work for certain strains of Aβ that exhibit conformations similar to those against which the mAb was raised. Several clinical trials involving Aβ mAbs have produced disappointing results (53). Although these antibodies may have been administered too late in the disease course to produce beneficial effects, Aβ strain heterogeneity in AD patients may have also contributed to their failure.

Materials and Methods

Additional methods are provided in *SI Materials and Methods*.

Human Tissue Samples. Frozen brain tissue samples (temporal cortex) were obtained from neuropathologically confirmed cases of AD. The Swedish mutant sample (Braak stage V–VI with CAA and a minor cerebellar hemorrhage) was obtained from a 61-y-old female, and the Arctic mutant sample (Braak stage V–VI with CAA and no other copathology) was obtained from a 64-y-old male. Two sporadic AD samples were used: case i (Braak stage V–VI with Lewy body copathology) was obtained from a 62-y-old male, and case ii (Braak stage V–VI with no other copathology) was obtained from an 85-y-old female. Control brain tissue was obtained from the frontal cortex of a 79-y-old male who did not exhibit any clinical or pathological signs of a neurodegenerative disease. Levels of various Aβ peptides in the individual brain samples are shown in Table S1.

Mice. Tg(APP23) mice, which express human APP (751-aa isoform) containing the Swedish mutation under the control of the *Thy-1.2* promoter (35), were maintained on a C57BL/6 background. Tg(*Gfap*-luc) mice, which express firefly luciferase under the control of the murine *Gfap* promoter (36), were a gift from Caliper Life Sciences (Alameda, CA) and maintained on an FVB/N background. To create bigenic Tg(APP23:*Gfap*-luc) mice, hemizygous Tg(APP23) mice were crossed with homozygous Tg(*Gfap*-luc) animals. All animal experiments were performed under protocols approved by the Institutional Animal Care and Use Committee at the University of California.

Neuropathology. Female mice were euthanized but not perfused before brain removal. Brains were then immersion-fixed in 10% (vol/vol) buffered

Watts et al.

www.manaraa.com

formalin followed by embedding in paraffin using standard procedures. Sections were cut at 8 μm, mounted on glass slides, deparaffinized, and then processed for immunohistochemistry. Endogenous tissue peroxidases were inhibited by incubating the slides in 3% hydrogen peroxide solution for 30 min, and sections to be stained with anti-Aβ antibodies were pretreated with formic acid for 5 min. Slides were blocked with 10% (vol/vol) normal goat serum for 1 h and then incubated with primary antibody overnight at 4 °C. The following primary antibodies were used: anti-Aβ mouse mAb 4G8 (1:250 dilution; Covance), anti-Aβ40 mouse mAb 11A50-B10 (1:200 dilution; Covance), anti-Aβ38 rabbit mAbs BA1-13 (1:200 dilution; Covance) and 7-14-4 (1:250 dilution; Covance), anti-collagen IV rabbit polyclonal antibody ab6586 (1:500 dilution; Abcam), and anti-GFAP rabbit polyclonal antibody Z0334 (1:500 dilution; Dako). Bound antibody was detected using a Vectastain ABC Peroxidase Kit (Vector Laboratories) and visualized using 3–3′-diaminobenzidine. Slides were counterstained with hematoxylin and then photographed using an AxioImager.A1 microscope (Carl Zeiss). For fluorescent double-labeling experiments, secondary antibodies conjugated to AlexaFluor 488, 568, or 647 (Life Technologies) were used. For Aβ/collagen IV double stains, sections were first pretreated with formic acid and then autoclaved in citrate buffer for epitope retrieval. All fluorescently labeled samples were visualized using a Leica SP8 confocal microscope.

1. Hardy J, Selkoe DJ (2002) The amyloid hypothesis of Alzheimer's disease: Progress and problems on the road to therapeutics. *Science* 297(5580):353–356.
2. Braak H, Braak E (1991) Neuropathological stageing of Alzheimer-related changes. *Acta Neuropathol* 82(4):239–259.
3. Jucker M, Walker LC (2013) Self-propagation of pathogenic protein aggregates in neurodegenerative diseases. *Nature* 501(7465):45–51.
4. Guo JL, Lee VM (2014) Cell-to-cell transmission of pathogenic proteins in neurodegenerative diseases. *Nat Med* 20(2):130–138.
5. Prusiner SB (1982) Novel proteinaceous infectious particles cause scrapie. *Science* 216(4542):136–144.
6. Wickner RB (1994) [URE3] as an altered URE2 protein: Evidence for a prion analog in *Saccharomyces cerevisiae*. *Science* 264(5158):566–569.
7. Si K, Lindquist S, Kandel ER (2003) A neuronal isoform of the aplysia CPEB has prion-like properties. *Cell* 115(7):879–891.
8. Prusiner SB (2012) Cell biology. A unifying role for prions in neurodegenerative diseases. *Science* 336(6088):1511–1513.
9. Ashe KH, Aguzzi A (2013) Prions, prionoids and pathogenic proteins in Alzheimer disease. *Prion* 7(1):55–59.
10. Hardy J, Revesz T (2012) The spread of neurodegenerative disease. *N Engl J Med* 366(22):2126–2128.
11. Thal DR, Rüb U, Orantes M, Braak H (2002) Phases of Aβ-deposition in the human brain and its relevance for the development of AD. *Neurology* 58(12):1791–1800.
12. Meyer-Luehmann M, et al. (2006) Exogenous induction of cerebral beta-amyloidogenesis is governed by agent and host. *Science* 313(5794):1781–1784.
13. Eisele YS, et al. (2010) Peripherally applied Abeta-containing inoculates induce cerebral beta-amyloidosis. *Science* 330(6006):980–982.
14. Watts JC, et al. (2011) Bioluminescence imaging of Abeta deposition in bigenic mouse models of Alzheimer's disease. *Proc Natl Acad Sci USA* 108(6):2528–2533.
15. Morales R, Duran-Aniotz C, Castilla J, Estrada LD, Soto C (2012) *De novo* induction of amyloid-β deposition *in vivo*. *Mol Psychiatry* 17(12):1347–1353.
16. Stöhr J, et al. (2012) Purified and synthetic Alzheimer's amyloid beta (Aβ) prions. *Proc Natl Acad Sci USA* 109(27):11025–11030.
17. Rosen RF, et al. (2012) Exogenous seeding of cerebral β-amyloid deposition in βAPP-transgenic rats. *J Neurochem* 120(5):660–666.
18. Bessen RA, et al. (1995) Non-genetic propagation of strain-specific properties of scrapie prion protein. *Nature* 375(6533):698–700.
19. Telling GC, et al. (1996) Evidence for the conformation of the pathologic isoform of the prion protein enciphering and propagating prion diversity. *Science* 274(5295):2079–2082.
20. Tanaka M, Chien P, Naber N, Cooke R, Weissman JS (2004) Conformational variations in an infectious protein determine prion strain differences. *Nature* 428(6980):323–328.
21. Petkova AT, et al. (2005) Self-propagating, molecular-level polymorphism in Alzheimer's beta-amyloid fibrils. *Science* 307(5707):262–265.
22. Kodali R, Williams AD, Chemuru S, Wetzel R (2010) Abeta(1-40) forms five distinct amyloid structures whose β-sheet contents and fibril stabilities are correlated. *J Mol Biol* 401(3):503–517.
23. Nilsson KP, et al. (2007) Imaging distinct conformational states of amyloid-beta fibrils in Alzheimer's disease using novel luminescent probes. *ACS Chem Biol* 2(8):553–560.
24. Paravastu AK, Qahwash I, Leapman RD, Meredith SC, Tycko R (2009) Seeded growth of beta-amyloid fibrils from Alzheimer's brain-derived fibrils produces a distinct fibril structure. *Proc Natl Acad Sci USA* 106(18):7443–7448.
25. Lu JX, et al. (2013) Molecular structure of β-amyloid fibrils in Alzheimer's disease brain tissue. *Cell* 154(6):1257–1268.
26. Mayeux R, Stern Y, Spanton S (1985) Heterogeneity in dementia of the Alzheimer type: Evidence of subgroups. *Neurology* 35(4):453–461.
27. Nilsberth C, et al. (2001) The 'Arctic' APP mutation (E693G) causes Alzheimer's disease by enhanced Abeta protofibril formation. *Nat Neurosci* 4(9):887–893.
28. Lashuel HA, et al. (2003) Mixtures of wild-type and a pathogenic (E22G) form of Aβ40 in vitro accumulate protofibrils, including amyloid pores. *J Mol Biol* 332(4):795–808.
29. Philipson O, et al. (2012) The Arctic amyloid-β precursor protein (AβPP) mutation results in distinct plaques and accumulation of N- and C-truncated Aβ. *Neurobiol Aging* 33:1010.e1–1010.e13.
30. Kalimo H, et al. (2013) The Arctic AβPP mutation leads to Alzheimer's disease pathology with highly variable topographic deposition of differentially truncated Aβ. *Acta Neuropathol Commun* 1(1):60.
31. Citron M, et al. (1992) Mutation of the β-amyloid precursor protein in familial Alzheimer's disease increases β-protein production. *Nature* 360(6405):672–674.
32. Mullan M, et al. (1992) A pathogenic mutation for probable Alzheimer's disease in the APP gene at the N-terminus of beta-amyloid. *Nat Genet* 1(5):345–347.
33. Lannfelt L, et al. (1994) Amyloid precursor protein mutation causes Alzheimer's disease in a Swedish family. *Neurosci Lett* 168(1-2):254–256.
34. Peretz D, et al. (2001) Strain-specified relative conformational stability of the scrapie prion protein. *Protein Sci* 10(4):854–863.
35. Sturchler-Pierrat C, et al. (1997) Two amyloid precursor protein transgenic mouse models with Alzheimer disease-like pathology. *Proc Natl Acad Sci USA* 94(24):13287–13292.
36. Zhu L, et al. (2004) Non-invasive imaging of GFAP expression after neuronal damage in mice. *Neurosci Lett* 367(2):210–212.
37. Jucker M (2010) The benefits and limitations of animal models for translational research in neurodegenerative diseases. *Nat Med* 16(11):1210–1214.
38. Heilbronner G, et al. (2013) Seeded strain-like transmission of β-amyloid morphotypes in APP transgenic mice. *EMBO Rep* 14(11):1017–1022.
39. Rönnbäck A, et al. (2011) Progressive neuropathology and cognitive decline in a single Arctic APP transgenic mouse model. *Neurobiol Aging* 32(2):280–292.
40. Moro ML, et al. (2012) *APP* mutations in the Aβ coding region are associated with abundant cerebral deposition of Aβ38. *Acta Neuropathol* 124(6):809–821.
41. Gabizon R, et al. (1996) Insoluble wild-type and protease-resistant mutant prion protein in brains of patients with inherited prion disease. *Nat Med* 2(1):59–64.
42. Chen SG, et al. (1997) Allelic origin of the abnormal prion protein isoform in familial prion diseases. *Nat Med* 3(9):1009–1015.
43. Parchi P, et al. (1998) Different patterns of truncated prion protein fragments correlate with distinct phenotypes in P102L Gerstmann-Sträussler-Scheinker disease. *Proc Natl Acad Sci USA* 95(14):8322–8327.
44. Benilova I, Karran E, De Strooper B (2012) The toxic Aβ oligomer and Alzheimer's disease: An emperor in need of clothes. *Nat Neurosci* 15(3):349–357.
45. Stöhr, et al. (2014) Distinct synthetic Aβ prion strains producing different amyloid deposits in bigenic mice. *Proc Natl Acad Sci USA* 111:10329–10334.
46. Hendriks L, et al. (1992) Presenile dementia and cerebral haemorrhage linked to a mutation at codon 692 of the β-amyloid precursor protein gene. *Nat Genet* 1(3):218–221.
47. Schmidt C, et al. (2011) Rapidly progressive Alzheimer disease. *Arch Neurol* 68(9):1124–1130.
48. Guo JL, et al. (2013) Distinct α-synuclein strains differentially promote tau inclusions in neurons. *Cell* 154(1):103–117.
49. Watts JC, et al. (2013) Transmission of multiple system atrophy prions to transgenic mice. *Proc Natl Acad Sci USA* 110(48):19555–19560.
50. Clavaguera F, et al. (2013) Brain homogenates from human tauopathies induce tau inclusions in mouse brain. *Proc Natl Acad Sci USA* 110(23):9535–9540.
51. Berry DB, et al. (2013) Drug resistance confounding prion therapeutics. *Proc Natl Acad Sci USA* 110(44):E4160–E4169.
52. Klunk WE, et al. (2005) Binding of the positron emission tomography tracer Pittsburgh compound-B reflects the amount of amyloid-β in Alzheimer's disease brain but not in transgenic mouse brain. *J Neurosci* 25(46):10598–10606.
53. Delrieu J, Ousset PJ, Caillaud C, Vellas B (2012) 'Clinical trials in Alzheimer's disease': Immunotherapy approaches. *J Neurochem* 120(Suppl 1):186–193.